Society For Biomaterials

In vitro and *in vivo* experiments with iron oxide nanoparticles functionalized with DEXTRAN or polyethylene glycol for medical applications: Magnetic targeting

M. L. Mojica Pisciotti,[1] E. Lima Jr.,[1] M. Vasquez Mansilla,[1] V. E. Tognoli,[1] H. E. Troiani,[2] A. A. Pasa,[3] T. B. Creczynski-Pasa,[4] A. H. Silva,[4] P. Gurman,[5] L. Colombo,[6] G. F. Goya,[7] A. Lamagna,[5] R. D. Zysler[1]

[1]Div. Resonancias Magnéticas, Centro Atómico Bariloche/CONICET, S. C. Bariloche 8400, Argentina
[2]Div. Física de Metales, Centro Atómico Bariloche/CONICET, S. C. Bariloche 8400, Argentina
[3]Depto. de Física, Universidade Federal de Santa Catarina, Florianópolis, 88040-900, Brazil
[4]Depto. de Ciências Farmacêuticas, Universidade Federal de Santa Catarina, Florianópolis 88040-900, Brazil
[5]Depto. de Micro y Nanotecnologia, Centro Atómico Constituyentes, San Martin 1650, Argentina
[6]Instituto de Oncología A.H. Roffo, UBA/CONICET/CAECIHS (UAI), Av. San Martín 5481, (1417) CABA, Argentina
[7]Instituto de Nanociencia de Aragón, Universidad de Zaragoza, Zaragoza 50018, Spain

Received 16 May 2013; revised 13 September 2013; accepted 20 October 2013
Published online 23 January 2014 in Wiley Online Library (wileyonlinelibrary.com). DOI: 10.1002/jbm.b.33068

ABSTRACT: In this research work, DEXTRAN- and polyethylene glycol (PEG)-coated iron-oxide superparamagnetic nanoparticles were synthetized and their cytotoxicity and biodistribution assessed. Well-crystalline hydrophobic Fe_3O_4 SPIONs were formed by a thermal decomposition process with $d = 18$ nm and $\sigma = 2$ nm; finally, the character of SPIONs was changed to hydrophilic by a post-synthesis procedure with the functionalization of the SPIONs with PEG or DEXTRAN. The nanoparticles present high saturation magnetization and superparamagnetic behavior at room temperature, and the hydrodynamic diameters of DEXTRAN- and PEG-coated SPIONs were measured as 170 and 120 nm, respectively. PEG- and DEXTRAN-coated SPIONs have a Specific Power Absorption SPA of 320 and 400 W/g, respectively, in an ac magnetic field with amplitude of 13 kA/m and frequency of 256 kHz. *In vitro studies* using VERO and MDCK cell lineages were performed to study the cytotoxicity and cell uptake of the SPIONs. For both cell lineages, PEG- and DEXTRAN-coated nanoparticles presented high cell viability for concentrations as high as 200 μg/mL. *In vivo* studies were conducted using BALB/c mice inoculating the SPIONs intravenously and exposing them to the presence of an external magnet located over the tumour. It was observed that the amount of PEG-coated SPIONs in the tumor increased by up to 160% when using the external permanent magnetic as opposed to those animals that were not exposed to the external magnetic field. © 2014 Wiley Periodicals, Inc. J Biomed Mater Res Part B: Appl Biomater, 102B: 860–868, 2014.

Key Words: SPIONS quantification, tumors, SPIONs biodistribution, magnetic nanoparticles, hyperthermia, SPIONS biocompatibility, cell uptake, superparamagnetism, mice

How to cite this article: Mojica Pisciotti ML, Lima E Jr, Vasquez Mansilla M, Tognoli VE, Troiani HE, Pasa AA, Creczynski-Pasa TB, Silva AH, Gurman P, Colombo L, Goya GF, Lamagna A, Zysler RD. 2014. *In vitro* and *in vivo* experiments with iron oxide nanoparticles functionalized with DEXTRAN or polyethylene glycol for medical applications: Magnetic targeting. J Biomed Mater Res Part B 2014:102B:860–868.

INTRODUCTION

Recent advances in nanotechnology are expected to revolutionize the field of medical therapeutics; among these technologies, superparamagnetic iron-oxide nanoparticles (SPIONs) appear as a promising field in many therapeutic areas. The potential of SPIONs to transport drugs to a specific site of the organism by taking advantage of its capacity to be manipulated by an external magnetic field, thus avoiding potentially adverse reactions caused by unspecific binding of the drug to healthy tissues and as a therapeutic tool themselves have encouraged these studies and developed commercial products based on SPIONs.[1] Lubbe et al. in 1996[2] have successfully used SPIONs in the first clinical trial reported, and after that, the use of these systems for therapeutics have been studied intensively. Following this line, toxicological studies of SPIONs are urgently needed to determine its effects in human health.[3]

A promising therapeutic application of SPIONs is in the magnetic fluid hyperthermia, which consists in the heating

Correspondence to: E. Lima, Jr. (e-mail: lima@cab.cnea.gov.ar)
Contract grant sponsors: CONICET, ANPCyT, Universidad de Cuyo, CNEA, CNPq (Conselho Nacional de Desenvolvimento Científico e Tecnológico), CAPES (Coordenação de Aperfeiçoamento de Pessoal de Nível Superior), and FAPESC (Fundação de Amparo à Pesquisa de Santa Catarina) as well as for REUNI/MEC Program for the Pharmacy doctoral degree fellowship (A. H. Silva)

of the target tissue by the nanoparticles when exposed to an external magnetic field. In this way, the SPIONs can be used to destroy tumors by cell hyperthermia,[4]. It is evident that this kind of technique offers a wide range of benefits over virtually any other therapeutic approach because several features of SPIONs can be controlled, including functionalization of their surface to control specific binding to different cancer cells types and controlled pharmacokinetics by magnetic manipulation. Moreover, the SPIONs can be used simultaneously as contrast agent, thus detecting and treating a disease in real time.[5,6]

Proper delivery of the SPIONs to the target tissue results critical for their clinical application to avoid broad biodistribution and damage to healthy tissues. Therefore, a comprehensive understanding of the biodistribution of SPIONs throughout the body is mandatory. To achieve this goal, different kinds of analytical methods, including qualitative and quantitative ones, have been developed to assess the presence of SPION in animal tissues by means of *in vitro* or *in vivo* assays.[7–17] Although the mechanism of SPIONs uptake by different cell types is still under investigation, a great amount of experimental work supports the hypothesis that the influence of the coating layer is a key factor.[16,18] Furthermore, a vast amount of experiments involving an enormous variety of chemical coatings have been performed, reporting their influence on the biological response in both cases, *in vitro* (cytotoxicity) and *in vivo* (biocompatibility).[19–22] Despite the large number of experiments conducted, the biodistribution and fate of SPIONs in the human body is still not well understood and more experimental data are needed.

In this work, we have performed *in vitro* and *in vitro* experiments with SPIONs of 18 nm and narrow size dispersion. The SPIONs were functionalized with polyethylene glycol (PEG) and DEXTRAN (a complex, branched glycan composed of chains of different lengths). We morphologically, magnetically, and rheologically characterized the SPIONs, while the Specific Power Absorption of the SPIONs was determined for a bio-friendly ac magnetic field. *In vitro* experiments were performed to test the cytotoxicity of these systems as well as the cell uptake by VERO and MDCK lineages. *In vivo* experiments consist in determining the ability to concentrate SPIONs in a tumor with a magnetic-assisted delivery and comparing the amount of SPIONs in the tumor with that in other organs of Balb/c mice. To the best of our knowledge, the potential biological and medical applications of SPIONs with these coatings and produced by this route of synthesis have not yet been reported. In addition, the behaviour of the PEG-coated SPIONs in the magnetic-assisted delivery experiment is very promising.

MATERIALS AND METHODS

SPION preparation

The most common method for preparation of iron oxide nanoparticles is co-precipitation, but this process generally, needs additional steps to purify and reduce the obtained size distribution.[23] Conversely, there is a more effective process based on decomposition of iron precursors to synthesize the iron oxide core coated with a layer of oleic acid in a single step.[24] This method results in hydrophobic nanoparticles, requiring a post-synthesis procedure to make them hydrophilic.[25] The nanoparticles are suspended in an aqueous media and functionalized if necessary. This latter method yields to narrow particle size distribution with an easily controlled mean diameter, which are desirable features.[26] This method was used to improve the quality of SPIONs and to control their morphology.

Nanoparticles were prepared by thermal decomposition of iron(III) acetylacetonate ($Fe(acac)_3$) in the presence of oleic acid and working at reflux condition during 15 min, with using as solvent trioctylamine (boiling point 630 K). The size of the particles was tailored by the surfactant:precursor molar ratio ([Surf.]:[Prec.]) and the total synthesis time, aimed to obtain a 18 nm size nanoparticles. The as-prepared sample consisted of a black suspension in a non-polar solvent of ferrite nanoparticles coated with an oleic acid monolayer. To use these nanoparticles for biological applications they were coating with 11-Aminoundecanoic acid tetramethylammonium salt (11-AATS) as already described in the literature.[25] Briefly, the oleic acid-coated nanoparticles and the 11-AATS were diluted in dichloromethane (0.1 wt %). The mixture was sonicated in an ultrasound bath for 1 h and after an incubation time of 24 h the nanoparticles became hydrophilic. Thus, PEG and DEXTRAN molecules could be attached in the nanoparticles.[27,28] Finally, a stable biocompatible aqueous suspension of PEG- or DEXTRAN coated SPIONs was obtained.

Experimental details

Magnetic nanoparticles were characterized by transmission electron microscopy (TEM) operating at 200 kV (Philips CM 200 electron microscope). TEM specimens were prepared by dropping the ferrofluid containing the nanoparticles in a copper grid covered with a carbon thin film. X-ray diffraction (XRD) patterns were collected in θ-2θ geometry with a Philips W1700 diffractometer, using Cu–Kα radiation. Magnetization measurements as a function of magnetic field (-10 to 10 kOe) were performed using a commercial vibrating sample magnetometer (VSM—Lakeshore) at room temperature. Magnetization measurements as function of temperature were performed in a commercial SQUID magnetometer (Quantum Design).

Hydrodynamic radius was measured by light scattering in a ZetaSizer 1000 (Malvern Instruments) with the nanoparticles dispersed in toluene or water, depending on the coating, at very low concentrations. Each sample was measured about 10 times to determine the mean diameter value. The Fourier transform infra-red (FTIR) spectra were collected in a commercial spectrometer (Frontier Perker-Elmer FT-IR Spectrometers) with range from 400 to 4000 nm. The samples for FTIR measurements were conditioned by two ways depending of the solvent of the nanoparticles. For the hydrophobic particles, a disk of potassium bromide was prepared and the nanoparticles with the inorganic oil were put on the disk. For the hydrophilic particles, the aqueous solution was saturated with potassium bromide and the water

was vaporized in a heater, and the final powder was pressed in a hydraulic press.

Experimental SPA measurements were made placing 0.5–1 mL aliquots of SPIONs into the working space where an alternating magnetic field was generated using a home-made ac-field generator. The ac generator, consisting of a resonant LC tank working close to the resonant frequency, was used to measure the specific power absorption (SPA) of the samples. A magnetic field (f = 256 kHz, H = 13 kA/m) was achieved inside the coil. The temperature data were measured using a fiber-optic temperature probe (ReflexTM, Neoptix) that was unaffected by the ac magnetic field. The SPA values were obtained from the initial slope of the heating curves measured inside an insulated Dewar. The experiments were performed with colloids having around 0.5 % w/v as standard concentration of SPIONs for all samples, with the nanoparticles dispersed in water.

In vitro experiments

Cytotoxicity assays were evaluated measuring cell viability of VERO and MDCK cell lines after 24 h of incubation with PEG- and DEXTRAN-coated nanoparticles at different concentrations. Cell viability was assessed by the 3-[4,5-dimethylthiazol-2-yl]-2,5-diphenyltetrazolium bromide (MTT) assay[29] that measures the integrity of the mitochondrial function. The optical absorption was measured at 540 nm and it was compared with the intensity in a control group cultured without the nanoparticles considered to have 100% viability. In total, each experiment was performed with 10,000 cells in average, and the viability was assessed as a function of the concentration of the SPIONs in the medium (μg of SPIONs per mL of medium—μg/mL). Fibroblast cell lines have been used to determine toxic effects induced by nanoparticles as they are the major cellular constituent of fibrous connective tissue, and Vero and MDCK cells have frequently been used with cytotoxicity assays with the advantages of fast grown and easy access.[30–32]

In vivo experiments

In vivo assays were conducted using a syngeneic transplant animal model consisting in BALB/c mice aged 11 weeks. *In vivo* assays were conducted using a syngeneic tumor animal model. 9 weeks old BALB/c mice, were inoculated subcutaneously in the left flank with 200.000 cells of the syngeneic murine mammary adenocarcinoma tumor cell line LM3.

After 2 weeks, when tumors were clearly visible, the animals were injected with 200 μL of an aqueous suspension containing DEXTRAN- and PEG-coated magnetite nanoparticles 0.5% *m/v* in the tail vein, to observe the effects of an external dc magnetic field on the amount of the nanoparticles absorbed in different organs: liver, lung, tumor, and skin tissues (ipsilateral and contralateral). The magnetic field was produced by a permanent magnet: a circular FeNdB magnet with 5 mm of diameter and 2 mm of thickness: ∼10 kOe at the surface. The magnet was placed on the skin of the left side that was the region where the tumor was implanted. In total, five groups of six animals each one were organized as follow: Group 1: PEG-coated SPIONs with magnet; Group 2: PEG-coated SPIONs without magnet; Group 3: DEXTRAN-coated SPIONs with magnet; Group 4: DEXTRAN-coated SPIONs without magnet; and the control group: not exposed to the SPIONs.

After 24 h of the injection, the animals were euthanized. The magnet was localized on the tumor during 24 h. All procedures involving animals were performed following NIH guidelines for animal care. Liver, lung, tumor, and skin tissues (ipsilateral and contralateral with respect to the tumor) were extracted and fixed in formalin solution for 48 h and then through a series of ethanol solutions with 70, 96, and 100% *v/v* successively. The amount of SPIONs in the *ex vivo* tissues was obtained by means of magnetization measurements, using the superparamagnetic characteristics of the system, as described elsewhere.[17]

RESULTS

Morphological and magnetic characterization of SPIONs

TEM and high-resolution TEM (HRTEM) images of SPIONs are presented in Figure 1(a,b), respectively. Nanoparticles presented spherical-like shape and a narrow Gaussian size distribution with mean diameter $< d > = 18$ nm and dispersion $\sigma = 2$ nm, as obtained from the fitting of the diameter histogram presented in the inset of Figure 1(a). HRTEM image evidenced the high crystallinity of the nanoparticles (atomic planes are clearly observed in the whole particle) and the fast Fourier transformation (FFT) of the image [see inset of Figure 1(b)] confirms the crystalline structure expected for the spinel structure of the ferrite (magnetite Fe_3O_4 and maghemite γ-Fe_2O_3). Figure 1(c) presents the XRD profile, where the peaks associated with the crystalline reflections of the planes of spinel structure are observed, corroborating the crystallinity observed in HRTEM images. According to the Scherrer's formula, which gives the crystallite size from the peak width, the mean grain size of our sample is about 15 nm.

Figure 2(a) displays the $M(T)$ curves measured in ZFC and FC conditions. These curves clearly show an irreversibility temperature at T_{Irr} = 280 K and the ZFC curve exhibits a maximum temperature at T_{Max} = 190 K, which are associated to the highest blocking temperature (T_B) for the system and the average one, respectively. Above these temperatures, the system is superparamagnetic. Therefore, these SPIONs are, indeed, superparamagnetic at room temperature for the time range of dc measurements. In fact, $M(H)$ curve measured at 300 K [see Figure 2(b)] presents no hysteresis, as expected for the superparamagnetic regime and it is well-fitted with the Langevin function, in opposition to the $M(H)$ curve measured at 5 K ($T << T_B$), also shown in Figure 2(b), which gives a coercive field of H_C = 200 Oe. Saturation Magnetization (M_S) value obtained from the $M(H)$ curves are 72 and 67 emu/g for 5 and 300 K, respectively. These values are similar to those observed for well-crystalline nanoparticles with equivalent diameter[33] and close to the M_S value of bulk material (92 emu/g),[34] and the reduction of saturation magnetization with increasing temperature is expected.

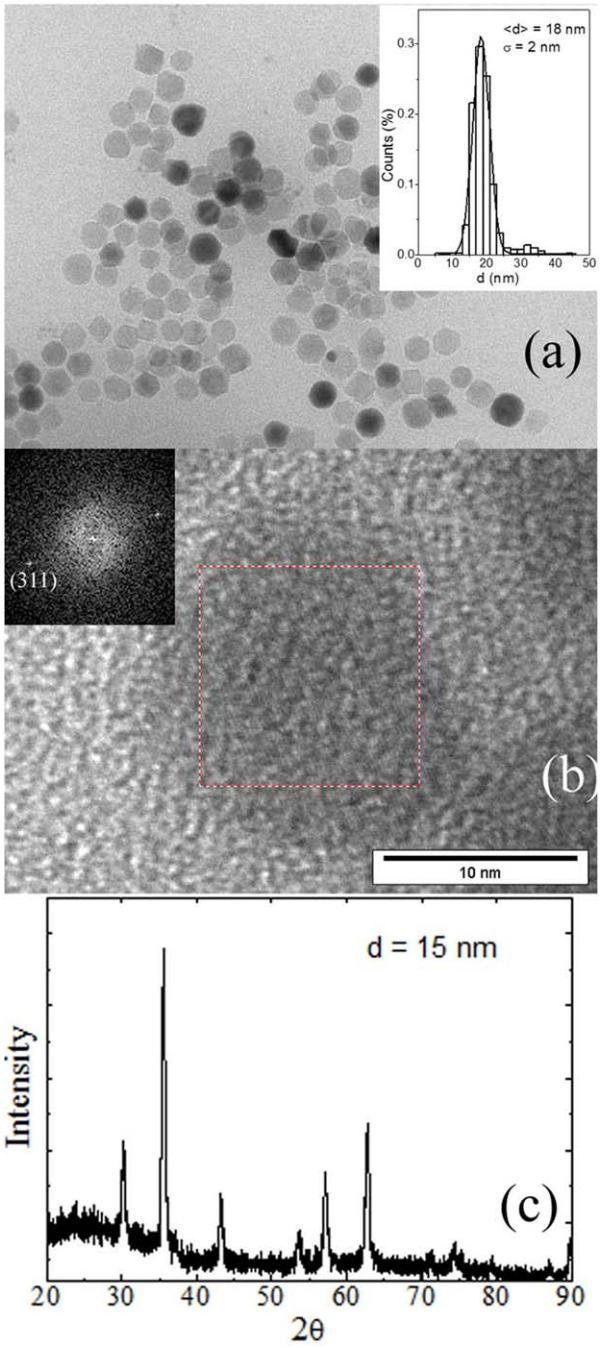

FIGURE 1. (a) TEM image; (b) HRTEM image; (c) XRD profile of the SPIONs. Inset of Figure 1(a) presents the histogram of diameters fitted with a Gaussian distribution (solid line). Inset of Figure 1(b) gives the FFT of the HRTEM image indexed as the (311) direction of the spinel structure of ferrite. [Color figure can be viewed in the online issue, which is available at wileyonlinelibrary.com.]

FTIR and hydrodynamic radius

According to light scattering measurements, the mean hydrodynamic diameter obtained for the oleic acid-coated nanoparticles was $<d_{hyd}> = 20 \pm 5$ nm, close to the mean diameter of the particles obtained from TEM images. For DEXTRAN- and PEG-coated nanoparticles dispersed in water $<d_{hyd}> = 170 \pm 70$ nm and $<d_{hyd}> = 120 \pm 40$ nm values were obtained, respectively. These values of $<d_{hyd}>$ are close to those observed in the literature for PEG- and DEXTRAN-coated superparamagnetic iron oxide nanoparticles,[19] despite the fact that hydrodynamic diameters of about 50 nm were also observed for iron-oxide nanoparticles coated with PEG and DEXTRAN.[35] We noted that the hydrodynamic diameter results critical for the performance of nanoparticles for drug delivery applications.[36] Specifically, for *in vivo* experiments, it is observed that nanoparticles larger than 80 nm are quickly uptaken by the reticuloendothelial system (RES) by macrophages in the liver and spleen.[37]

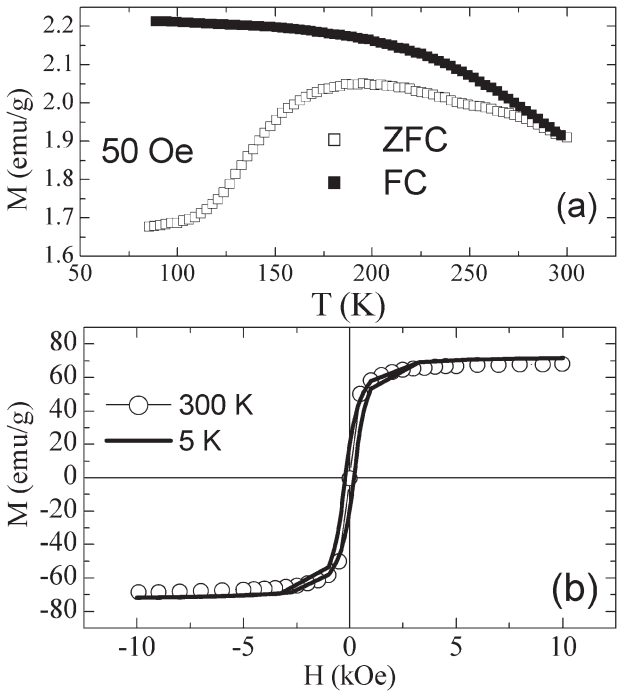

FIGURE 2. (a) *M*(*T*) curve of the SPIONs measured at ZFC and FC modes with $H = 100$ Oe; (b) *M*(*H*) curves of the SPIONs measured at 5 and 300 K.

Figure 3 exhibits the FTIR spectra of the SPIONs coated with oleic acid, PEG, and DEXTRAN. By comparing these experimental spectra with the reported values for the peak position of magnetite, oleic acid, PEG, and DEXTRAN, the contribution of each compound in the spectra was identified. For the as-prepared sample, the contribution of magnetite and oleic acid was observed, while for the other two samples, we observed the contributions of magnetite, together with PEG or DEXTRAN. Two characteristics of FTIR spectra of hydrophilic nanoparticles are interesting to remark. First, we do not observe the presence of 11-AATS; second, the FTIR spectra are in agreement with the literature for PEG- and DEXTRAN-coated nanoparticles.[38,39]

SPA measurements

Figure 4 shows the time dependence of the temperature of an aqueous-based ferrofluid containing our SPIONs with concentration of 0.5 wt % in the presence

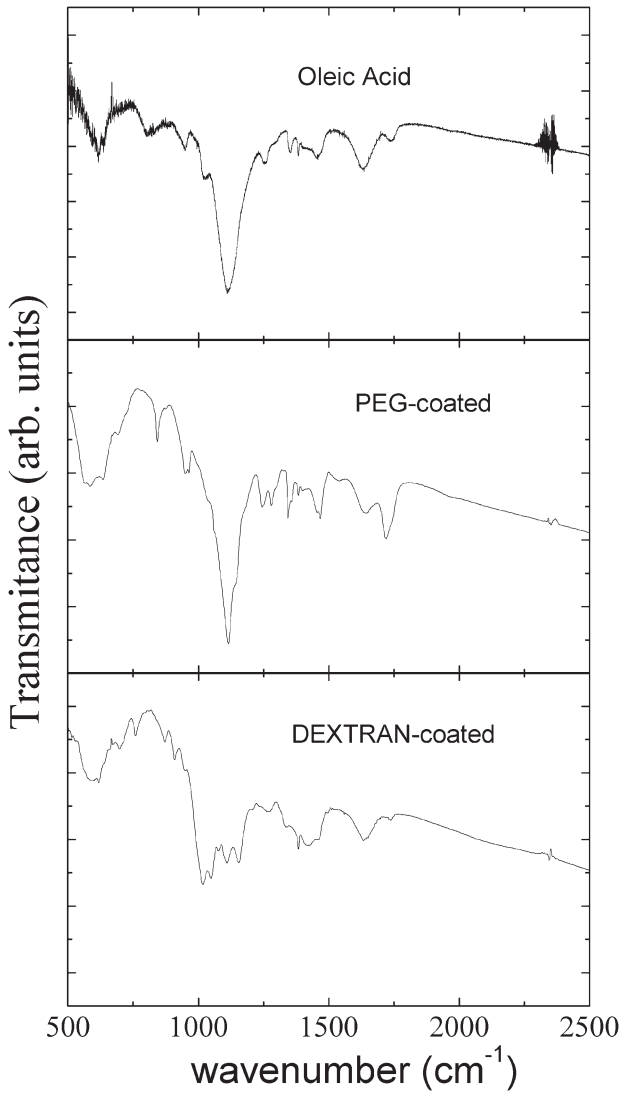

FIGURE 3. FTIR spectra of the samples composed by the as-prepared nanoparticles coated with oleic acid, and of those coated with PEG and DEXTRAN.

of an ac magnetic field with $H = 13$ kA/m and $f = 250$ kHz. We observed an increase of ~3.2°C and 2.5°C in only 10 s for the DEXTRAN- and PEG-coated SPIONs, respectively. SPA was obtained from the experimental time dependence of the temperature by the following expression:

$$\mathrm{SPA} = \left(\frac{c_{\mathrm{liq}} \cdot m_{\mathrm{liq}}}{m_{\mathrm{SPION}}}\right)\left(\frac{dT}{dt}\right), \qquad (1)$$

where c_{liq} is the specific heat of the water, m_{liq} and m_{SPION} are the mass of liquid and of SPIONs, respectively. Top panel of Figure 4 shows the derivative curve of the time dependence of the temperature of the ferrofluids containing DEXTRAN- and PEG-coated SPIONs, from which we calculated the respective SPA values of 400 and 320 W/g_{SPION} using the maximum values of the derivative curve for each sample.

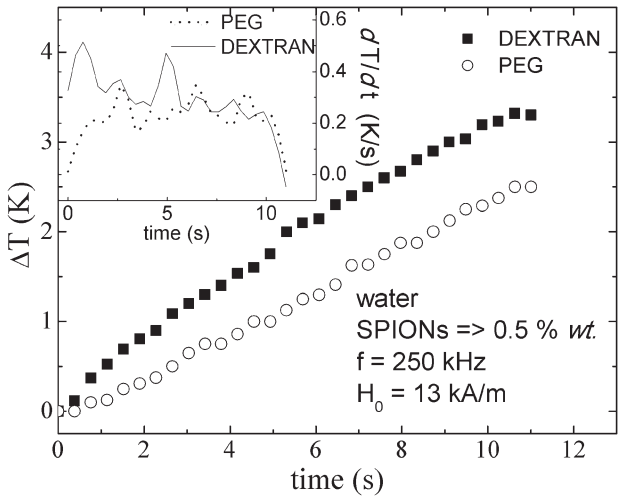

FIGURE 4. Time dependence of the temperature of water-based ferrofluids containing DEXTRAN- and PEG-coated SPIONs with concentration of 0.5 wt % for an applied field with $H = 13$ kA/m and $f = 250$ kHz. Inset gives the derivative curves used to calculate the SPA values for each sample.

In vitro tests

Figure 5 presents the cell viability measurements in VERO and MDCK cell lines exposed to different concentrations of ferrofluid containing the PEG- and DEXTRAN-coated SPIONs in the culture medium. Each point is the mean value obtained from distinct numbers of experiments for the concentration, and the corresponding error bar obtained is also presented. For the VERO cells treated with DEXTRAN-coated nanoparticles, viability was observed to be near 100% for concentrations as high as 300 μg/mL and this value decreased to ~75% for the concentration of 400 μg/mL. Viability of MDCK cells for DEXTRAN-coated SPIONs was close to 100% even for the concentration of 400 μg/mL. It was observed a different behavior for the PEG-coated SPIONs; if the error bar is considered, there is no mayor difference in the viability of both types of cell for 200 μg/mL (mean value close to 75%). However, cell viability decreases rapidly for higher concentrations, being lower than 50% for 400 μg/mL for both cell lineages. This significant difference among PEG- and DEXTRAN-coated nanoparticles for concentration higher than 200 μg/mL in both cell lineages remains even considering the error bar.

The high values of cell viability obtained for DEXTRAN-coated nanoparticles for VERO and MDCK cell lines were similar to those observed in the literature for nanoparticles with similar coating for human umbilical vein endothelial cells.[20] Our results evidenced no toxic effects of the 11-AATS used during the synthesis to produce hydrophilic nanoparticles. For higher concentration (>200 μg/mL), the values obtained for the PEG-coated SPIONs were lower than those observed in the literature[40] for high concentrations. This difference may be associated with two factors: first, in Choi et al.[40] primary cell cultures are used for the *in vitro* experiments; second, there the SPIONs were coated with a bilayer composed by the oleic acid (attached to the surface) and a commercial PEG-phospholipid conjugate, thus a

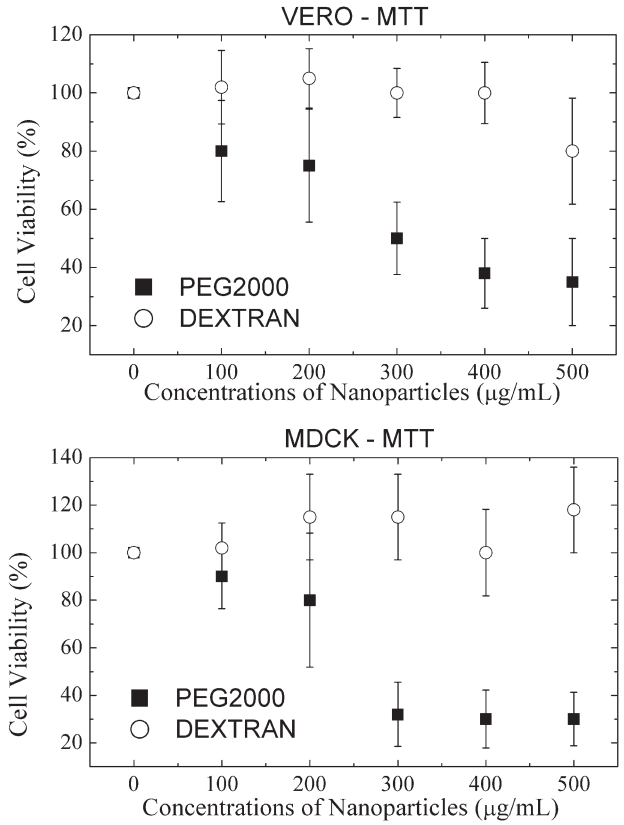

FIGURE 5. Cytotoxicity of nanoparticles in VERO and MDCK cell lineages by MTT assay. The cells were incubated with different concentrations of nanoparticles coated with PEG and DEXTRAN, for 24 h. The values are given in reference to the control population of cells (equivalent to 100%). Each point is the mean value obtained from distinct numbers of experiments for the concentration, and the corresponding bar obtained is also presented.

different coating was used in comparison with the one mentioned in this work. These two points may lead to the observed difference in the cytotoxicity for concentration >200 μg/mL.

It is important to note that cytotoxicity measurements obtained for DEXTRAN-coated SPIONs exhibited high cell viability even at concentrations as high as 200 μg/mL, indicating that the utilization of 11-AATS in the synthesis procedure does not induces a high toxicity for the systems. It is worth to say that interaction mechanisms between nanoparticles and living cells are complex and still not fully understood. There are many variables to consider when working with nanomaterials, including, besides the material, the size, shape, surface, charge, dispersion, agglomeration, and aggregation.[41]

Quantification of the amount of nanoparticles absorbed by the MDCK and VERO cell lines when incubated at high concentration (500 μg/mL) were performed by magnetic techniques. For these tests, DEXTRAN-coated nanoparticles were used because of the low *in vitro* cytotoxicity they present when there are high concentrations of this formulation. A quantity of 40 and 10 pg_{SPIONs}/cell was determined for VERO and MDCK cell lines, respectively, which have the same magnitude than those found in dendritic cells.[42]

Quantification of nanoparticles in different organs and in the tumor of BALB/c mice

In vivo experiments were performed to quantify the amount of PEG- and DEXTRAN-coated nanoparticles in the liver, lung, ipsilateral, and contralateral skin, and in the tumor for both situations: with and without the magnet. Table I shows the amount of nanoparticles found in each organ. The amounts are given in micrograms of nanoparticles per grams of *ex vivo* tissue after 24 h of the injection in the tail vein.

Three main results emerge from Table I. First, for both organic coatings and with or without the magnet, the majority of nanoparticles are localized in the lung and liver after 24 h, not in the tumor. Second, the amount of PEG-coated nanoparticles in the tumor with the presence of the magnet increases 160% in comparison to the group without the magnet. Finally, for DEXTRAN-coated nanoparticles no major difference was observed in the amount of nanoparticle in the tumor for both cases, with or without magnet. Another interesting observation is the low concentration of nanoparticles in the ipsilateral skin for both organic coatings, which is almost the same as the one observed for the contralateral skin even with the presence of the magnet. We have also observed that the amount of PEG-coated nanoparticles in the lung increases ~50% in the presence of the magnet.

DISCUSSION

Recent results in the literature[19] indicate that PEG-coated nanoparticles that have larger circulation time can be targeted to a brain tumor by applying a strong external magnetic field (2 kOe) in the tumor zone. The authors have

TABLE I. Amount of PEG-Coated and DEXTRAN-Coated Nanoparticles in Both Situation, With and Without Magnet, Detected by Magnetic Measurements in Different *Ex Vivo* Tissues of Injected BALB/c mice After 24 h

	PEG-coated (μg/g)		DEXTRAN-coated (μg/g)	
Tissue	With magnet (STD)	Without magnet (STD)	With magnet (STD)	Without magnet (STD)
Liver	1200 (70)	1565 (85)	1300 (81)	1357 (45)
Lung	5090 (430)	1572 (41)	2560 (64)	1679 (40)
Tumor	453 (30)	165 (5)	253 (9)	279 (20)
Contralateral skin	27 (8)	296 (10)	–	36 (5)
Ipsilateral skin	13 (5)	61 (5)	35 (5)	26 (5)

Each value corresponds to the mean value of six measurements and the number in the parenthesis corresponds to the respective standard deviation (STD).

observed a reduction in the nanoparticle concentration in the liver and spleen in comparison to those for other nanoparticle systems. They have also obtained an enhanced concentration of nanoparticles in the brain tumor (0.1% of the nanoparticles injected), confirming that an increase on the circulation time of the nanoparticles leads to a better magnetic targeting of a tissue. These results explain the poor efficiency that, until now, has been achieved by the use of a magnetic field gradient induced by an external magnet to mark a tumor for the delivery of PEG- and DEXTRAN-coated nanoparticles when injected in the vein tail of mice. In fact, the efficiency of the magnet to mark a target tissue depends on a larger circulation time of the nanoparticles.[36] In this regard, two key factors are the surface chemistry and the hydrodynamic diameter of the magnetic system. In this way, two options to increase the efficiency of the external magnetic field to concentrate the nanoparticles in the target are: (i) to inject the nanoparticles directly in the tumor, minimizing the effect of short circulation time; (ii) and/or to increase the circulation time with the reduction of the hydrodynamic diameter of the nanoparticles. Wang et al. studied the biodistribution of iron-oxide nanoparticles synthesized by coprecipitation in Wistar rats with a magnet localized on the abdominal area, close to the skin and immediately after the injection in the neck, the concentration of nanoparticles increased rapidly in the liver, lungs, and kidneys, similarly to the results provided here. However, when the magnet was positioned close to the injection zone, they observed different results, finding nanoparticles in the magnet zone. Thus, the injection of the nanoparticles into the artery that irrigate the tumor zone marked with the magnet may actually increase the efficiency of the procedure. Nevertheless, the presence of an external magnet limits the increase of the nanoparticles concentration close to the skin, and the injection of nanoparticles directly in the tumor is not an effective or possible technique for several biomedical procedures using drug delivery systems. At the same time, the reduction of hydrodynamic diameter could not be easily achieved since it is necessary to produce a smaller organic coating or to reduce the size of nanoparticles, which would lead to an increase in the interparticle interactions or to a detriment in their magnetic properties.[44] Finally, the use of chemical markers in the surface of nanoparticles attached to the PEG or DEXTRAN could provide a more efficient method for drug delivery, by increasing the amount of nanoparticles in the target tissue.[22,37]

According to *in vivo* experiments performed by the authors, the largest amount of nanoparticles were found in the lung and liver with or without magnet, probably as consequence of their morphological, chemical, and rheological characteristics. Similar results have already been observed for nanoparticles with PEG and DEXTRAN coatings and similar hydrodynamic diameter or even a smaller one.[19,45] This behavior is explained by the pharmacokinetics of these kinds of particles. When these particles are absorbed, biodistribution takes place mainly on the RES, which leads to a very high concentration of nanoparticles in liver and lungs, as well as in the spleen (the last one was not studied in this article). These phenomena could be explained to some extent to particle size and surface that makes SPIONs amenable to be uptake by macrophages of the RES.

However, it is observed a significant increase in the amount of PEG-coated SPIONs in the tumor with the magnet, an increase of 160 %. This result indicates a relative success in magnetic target of these SPIONs. In comparison, no increment was observed for the DEXTRAN-coated SPIONs. PEG-coated SPIONs have smaller hydrodynamic diameter and consequently a larger circulation time in comparison to the DEXTRAN-coated ones. It could be argued that the larger circulation time leads to a higher efficiency of the magnet to concentrate the nanoparticles in the tumor, although the larger amount of SPIONs was still detected in the lungs and in to a lesser extent in the spleen. The hydrodynamic diameter of the DEXTRAN-coated nanoparticles of 180 nm leads to a reduced circulation time, impairing the ability of the magnet to increase the concentration of the SPIONs at in the tumor site.

Interestingly, we have also observed a marked increase in the concentration of SPIONs in the lung, which was observed in all animals on these experimental conditions. This increase on the concentration of SPIONs in the lung, which was observed in all animals on these experimental conditions, cannot be easily understood and further studies are needed to fully understand the absorption mechanism of the SPIONs by the lung.

It is important to remark that the nanoparticles showed in this work are well-crystalline, with a mean diameter of 18 nm, a narrow size distribution of $\sigma = 2$ ($\sim$14%) and are coated with PEG and DEXTRAN. Additionally, the nanoparticles are superparamagnetic at room temperature, presenting high saturation magnetization and high magnetic susceptibility. The hydrodynamic diameters are 170 nm and 120 nm for the DEXTRAN- and PEG-coated systems, respectively. These characteristics make them interesting for biomedical applications. Cytotoxicity measurements indicate that the nanoparticles coated with PEG are non-toxic up to concentrations as high as 100 μg/mL, while the DEXTRAN-coated ones present low cytotoxicity even up to concentrations as high as 400 μg/mL, despite the use of 11-AATS in the synthesis. We also reinforce that the FTIR spectra of PEG- and DEXTRAN-coated SPIONS do not exhibit the peaks associated to 11-AATS. In addition, Ankamwar et al.[45] reported on the low cytotoxicity of Fe_3O_4 nanoparticles coated with 11-AATS at low concentration (about 100 μg/mL).

Although considering the potential application of DEXTRAN- and PEG-coated SPIONs for magnetic fluid hyperthermia, we have observed high SPA values: 420 W/g and 300 W/g, respectively. A potential medical application for SPIONs is the magnetic fluid hyperthermia, which consists in overheating a target tissue by the magnetic losses of a solution containing SPIONs in the presence of an external ac magnetic field.[46,47] The key parameter to determine the effectiveness of an ensemble of nanoparticles for magnetic hyperthermia is the SPA. The SPA depends of the morphological, magnetic (anisotropy and low-field magnetic susceptibility), and

rheological properties (hydrodynamic radius and formation of agglomerates) as well as the characteristic of the applied field (H and f). A high SPA leads to a lower exposition of the patient to the magnetic field and to the SPIONs as well as to a more efficient clinical procedure. Other important key to the success of the magnetic hyperthermia clinical protocol is the specific localization of the SPIONs in the tumor when one is capable of localizing the applied magnetic field on it. As a matter of fact, our DEXTRAN- and PEG-coated nanoparticles are able to produce the necessary heat to cause cell death by magnetic losses using ac magnetic field that represents no risk to the patient (see Ankamwar et al.[43] Maier-Hauff K. et al,[47] and Fortin J.-P. et al.[48] this ac applied magnetic field presents the value of $H.f = 10^6$ kA/m s, the same magnitude obtained for the magnetic field used in our experiments). To the best of our knowledge, these values of SPA are similar to the highest observed in the literature for chemical synthesized SPIONs.[49]

CONCLUSION

In this study, we report on the ability of *in vivo* enhancing of the uptake of PEG- and DEXTRAN-coated SPIONs by subcutaneous tumor cells by applying an external dc magnetic field. This field is obtained using a magnet implanted above the tumor site on the subcutaneous tissue of BALB/c mice after intravenous injection of the nanoparticles in the tail vein. In all *in vivo* experiments, we observe that the highest concentration of nanoparticles was found in liver and lung, one order of magnitude above the concentration in the tumor. Interestingly, we obtain a significant increment (about 160%) in the tumor uptake of the PEG-coated SPIONs in the presence of the magnetic field. Conversely, no change was observed in the tumor uptake of the DEXTRAN-coated SPIONs.

In addition, *in vitro* experiments of cytotoxicity and cell uptake involving VERO and MDCK cell lineages show that the PEG-coated SPIONs present low toxicity for concentrations as high as 200 μg/mL, while the DEXTRAN-coated SPIONs present low toxicity even for concentrations as high as 400 μg/mL. The cell uptake obtained for the DEXTRAN-coated SPIONs (500 μg/mL) were 40 and 10 pg_{SPIONs}/cell for VERO and MDCK lineages, respectively.

We remark that the method used to produce our nanoparticle allows us to obtain a system with controlled mean diameter, narrow sized distribution, and a high crystallinity. Consequently, the SPIONs present excellent and desirable magnetic properties for biomedical applications, specifically for drug delivery or magnetic fluid hyperthermia. For the later, it is worth to mention that SPA values of 320 and 400 W/g_{SPION} were obtained by the authors for PEG- and DEXTRAN coated SPION, respectively.

ACKNOWLEDGMENTS

The authors are thankful to the Laboratorio de Caracterización de Materiales (CAB-CNEA-Argentina) to the XRD profiles. M. L. Mojica Pisciotti thanks to ANPCyT and UNCuyo for her doctoral fellowship. The authors thank to Dr. Carlos Ramos for the critical reading of the manuscript.

REFERENCES

1. Bruton LL, Chabner BA, Knollmann BC. The Pharmacological Basis of Therapeutics. New York: Mc Graw Hill; 2011.
2. Lubbe AS, Bergemann C, Riess H, Shcriever F, Reichardt P, Possinger K, Matthias M, Dorken M, Herrmann F, Gurtler R, Haas N, Sohr R, Sander B, Lemke A-J, Olhendorf D, Huhnt W, Huhn D. Clinical Experiences with Magnetic Drug Targeting: A Phase I Study with 4′-Epidoxorubicin in 14 Patients with Advanced Solid Tumors. Cancer Res 1996;56:4686.
3. Jing Sun, Shaochuang Wang, Dong Zhao, Fei Han Hun, Lei Weng, Hui Liu. Cytotoxicity, permeability, and inflammation of metal oxide nanoparticles in human cardiac microvascular endothelial cells. Cell Biol Toxicol 2011;27:333–342.
4. Hilger I, Hergt R, Kaiser WA. Use of magnetic nanoparticle heating in the treatment of breast cancer. IEEE Proc Nanobiotechnol 2005;152:33.
5. McCarthy JR, Weisledder R. Multifunctional magnetic nanoparticles for targeted imaging and therapy. Adv Drug Delivery Rev 2008;60:1241.
6. Jung CW, Rogers JM, Groman VE. Lymphatic mapping and sentinel node location with magnetite nanoparticles. J Magn Magn Mater 1999;194:210.
7. Tate JA, Petryk AA, Giustini AJ, Hoopes PJ. In vivo biodistribution of iron oxide nanoparticles: an overview. Proc. SPIE 7901, Energy-based Treatment of Tissue and Assessment VI 2011;7901:790117.
8. Giustini AJ, Ivkov R, Hoopes PJ. Magnetic nanoparticle biodistribution following intratumoral administration. Nanotechnology 2011;22:345101.
9. Al Faraj A, Fauvelle F, Luciani N, Lacroix G, Levy M, Cremillieux Y, Canet-Soulas E. In vivo biodistribution and biological Impact of injected carbon nanotubes using magnetic resonance techniques. Int J Nanomedicine 2011;6:351–361.
10. Edwards D, Lewis J, Battle M, Lear R, Farrar G, Barnett DJ, Godden V, Oliveira A, Coombes C, Ahlstrom H. 99mTc-NC100668, a new tracer for imaging venous thromboemboli: pre-clinical biodistribution and incorporation into plasma clots in vivo and in vitro. Eur J Nucl Med Mol 2006;33:1258–1265.
11. Riemer J, Hoepken HH, Czerwinska H, Robinson SR, Dringen R. Colorimetric ferrozine-based assay for the quantization of iron in culture cells. Anal Biochem 2004;331:370.
12. Frank JA, Kalish H, Anderson SA, Jordan EK, Pawelczyk E, Arbab AS. Color transformation and fluorescence of Prussian blue-positive cells: implications for histologic verification of cells labeled with superparamagnetic iron oxide nanoparticles. Mol Imaging 2007;6:212.
13. Chertok B, Cole AJ, David AE, Yang VV. Comparison of electron spin resonance spectroscopy and plasma inductively-coupled plasma optical emission spectroscopy for biodistribution analysis of iron oxide nanoparticles. Mol Pharmaceutics 2010;7:375.
14. Stroh A, Faber C, Neuberger T, Lorenz P, Sieland K, Jakob PM, Webb A, Pilgrimm H, Schober R, Pohl EE, Zimmer C. *In vivo* detection limits of magnetically labeled embryonic stem cells in the rat brain using high-field (17.6 T) magnetic resonance imaging. Neuroimage 2005;24:635.
15. Bjornerud A, Johansson LO, Briley-Saebo K, Ahlstrom HK. Assessment of *T*1 and *T*2 effects *in vivo* and *ex vivo* using iron oxide nanoparticles in steady state-dependence in blood volume and water exchange. Magn Reson Med 2002;47:461.
16. Gamarra LF, Costa-Filho AJ, Mamani JB, Cassia Ruiz R, Pavon LF, Sibov TT, Vieira ED, Silva AC, Pontuschka WM, Amaro E, Jr. Ferromagnetic resonance for the quantification of superparamagnetic iron oxide nanoparticles in biological materials. Int J Nanomed 2010;5:203.
17. Zysler RD, Lima E Jr, Vasquez Mansilla M, Troiani HE, Mojica Pisciotti ML, Gurman P, Lamagna A, Colombo L. A New Quantitative Method to Determine the Uptake of SPIONs in Animal Tissue and Its Application to Determine the Quantity of Nanoparticles in the Liver and Lung of Balb-c Mice Exposed to the SPIONs. J Biomed Nanotechnol 2013;9:142–145.
18. Seong Cheol Hong, Jong Ho Lee, Jaewook Lee, Hyeon Yong Kim, Jung Youn Park, Johann Cho, Jaebeom Lee, Dong-Wook Han. Subtle cytotoxicity and genotoxicity differences in superparamagnetic iron oxide nanoparticles coated with various functional groups. Int J Nanomed 2011;6:3219–3231.

19. Cole AJ, David AE, Wang J, Galbán CJ, Yang VC. Magnetic brain tumor targeting and biodistribution of long-circulating PEG-modified, cross-linked starch-coated iron oxide nanoparticles. Biomaterials 2010;32:6291–6301.
20. Xinying Wu, Yanbin Tan, Hui Mao, Minming Zhang. Toxic effects of iron oxide nanoparticles on human umbilical vein endothelial cells. Int J Nanomed 2010;5:385–399.
21. Xinglu Huang, Linlin Li, Tianlong Liu, Nanjing Hao, Huiyu Liu, Dong Chen, Fangqiong Tang. The Shape Effect of Mesoporous Silica Nanoparticles on Biodistribution, Clearance, and Biocompatibility in Vivo. ACS Nano 2011;5:5390–5399.
22. Chertok B, David AE, Moffat BA, Yang VC. Substantiating in vivo magnetic brain tumor targeting of cationic iron oxide nanocarriers via adsorptive surface masking. Biomaterials 2009;30:6780.
23. Jarrett BR, Frendo M, Vogan J, Louie AY. Size-controlled synthesis of dextran sulfate coated iron oxide nanoparticles for magnetic resonance imaging. Nanotechnology 2007;18:035603.
24. Sun S, Zeng H. Size-Controlled Synthesis of Magnetite Nanoparticles. J Am Chem Soc 2002;124:8204.
25. Sun S, Zeng H, Robinson DB, Daoux S, Rice PM, Wang SX, Li G. Monodisperse MFe2O4 (M = Fe, Co, Mn) Nanoparticles. J Am Chem Soc 2004;126:273.
26. Vargas JM, Zysler RD. Tailoring the size in colloidal iron oxide magnetic nanoparticles. Nanotechnology 2005;16:1474.
27. Yi-Jing Zhang, Yen-Wen Lin, Chia-Chih Chang, Tzong-Ming Wu. Magnetic properties of hydrophilic iron oxide/polyaniline nanocomposites synthesized by in situ chemical oxidative polymerization. Synth Met 2010;160:1086–1091.
28. Zhang JL, Srivastava RS, Misra RDK. Core-Shell Magnetite Nanoparticles Surface Encapsulated with Smart Stimuli-Responsive Polymer: Synthesis, Characterization, and LCST of Viable Drug-Targeting Delivery System. Langmuir 2007;23:6342–6351.
29. Mosmann T. Rapid colorimetric assay for cellular growth and survival: application to proliferation and cytotoxicity assays. J Immunol Methods 1983;65:55–63.
30. Bouaziz C, Abid-Essefi S, Bouslimi A, El Golli E, Bacha H. Cytotoxicity and related effects of T-2 toxin on cultured Vero cells. Toxicon 2006;48:343–352.
31. Luque-Garcia JL, Sanchez-Díaz R, Lopez-Heras I, Camara C, Martin P. Bioanalytical strategies for in-vitro and in-vivo evaluation of the toxicity induced by metallic nanoparticles. TrAC Trends Anal Chem 2013;43:254–268.
32. Vaucher RA, Teixeira ML, Brandelli A. Investigation of the Cytotoxicity of Antimicrobial Peptide P40 on Eukaryotic Cells. Curr Microbiol 2010;60:1–5.
33. Lima E Jr, De Biasi E, Vasquez Mansilla M, Saleta ME, Effenberg F, Rossi LM, Cohen R, Rechenberg HR, Zysler RD. Surface effects in the magnetic properties of crystalline 3 nm ferrite nanoparticles chemically synthesized. J Appl Phys 2010;108:103919.
34. Smit J, Wijn HPJ. Ferrites. Eindhoven, The Netherlands: Philips' Technical Library; 1959.
35. Kodai Ujiie, Naoki Kanayama, Kei Asai, Mikio Kishimoto, Yusuke Ohara, Yoshimasa Akashi, Keiichi Yamada, Shinji Hashimoto, Tatsuya Oda, Nobuhiro Ohkohchi, Hideto Yanagihara, Eiji Kita, Masayuki Yamaguchi, Hirofumi Fujii, Yukio Nagasaki. Preparation of highly dispersible and tumor-accumulative, iron oxide nanoparticles Multi-point anchoring of PEG-b-poly(4-vinylbenzylphosphonate) improves performance significantly. Colloids Surf B 2011;88:771–778.
36. Heebeom Koo, Myung Sook Huh, In-Cheol Sun, Soon Hong Yuk, Kuiwon Choi, Kwangmeyung Kim, Ick Chan Kwon. In Vivo Targeted Delivery of Nanoparticles for Theranosis. Accounts Chem Res 2011;44:1018–1028.
37. Thorek DLJ, Chen AK, Czupryna J, Tsourkas A. Superparamagnetic Iron Oxide Nanoparticle Probes for Molecular Imaging. Ann Biomed Eng 2006;34:23–28.
38. Koneracka M, Zavisova V, Timko M, Kopcansky P, Tomasovicova N, Csach K. Magnetic properties of encapsulated magnetite in PLGA nanospheres. Acta Phys Pol A 2008;113:595–598.
39. Tomasovicova N, Koneracka M, Kopcansky P, Timko M, Zavisova V. Infrared study of biocompatible magnetic nanoparticles. Meas Sci Rev 2006;6:32–35.
40. Choi JY, Lee SH, Na HB, An K, Hyeon T, Seo TS. In vitro cytotoxicity screening of water-dispersible metal oxide nanoparticles in human cell lines. Bioprocess Biosyst Eng 2010;33:21–30.
41. Elsaesser A, Howard CV. Toxicology of nanoparticles. Adv Drug Deliv Rev 2012;64:129–137.
42. Marcos-Campos I, Asin L, Torres TE, Marquina C, Tres A, Ibarra MR, Goya GF. Cell death induced by the application of alternating magnetic fields to nanoparticle-loaded dendritic cells. Nanotechnology 2012;22:205101.
43. Yuh-Feng Wang, Chao-Ming Fu, Mei-Hua Chuang, Thau-Ming Cham, Mei-Ing Chung. Magnetically Directed Targeting Aggregation of Radiolabelled Ferrite Nanoparticles. J Nanomater 2011;1: 851520.
44. Lima E Jr, Brandl AL, Arelaro AD, Goya GF. Spin disorder and magnetic anisotropy in Fe3O4 nanoparticles. J Appl Phys 2005;99: 083908.
45. Ankamwar B, Lai TC, Huang JH, Liu RS, Hsiao M, Chen CH, Hwu YK. Biocompatibility of Fe3O4 nanoparticles evaluated by in vitro cytotoxicity assays using normal, glia and breast cancer cells. Nanotechnology 2010;21:075102.
46. Hilger I, Hiergeist R, Hergt R, Winnefeld K, Schubert H, Kaiser WA. Thermal Ablation of Tumors Using Magnetic Nanoparticles: An In Vivo Feasibility Study. Invest Radiol 2000;37:580–586.
47. Maier-Hauff K, Rothe R, Scholz R, Gneveckow U, Wust Pr, Thiesen B, Feussner A, von Deimling A, Waldoefner N, Felix R, Jordan A. Intracranial thermotherapy using magnetic nanoparticles combined with external beam radiotherapy: Results of a feasibility study on patients with glioblastoma multiforme. J Neurooncol 2007;81:53–60.
48. Fortin J-P, Gazeau F, Wilhelm C. Intracellular heating of living cells through Neel relaxation of magnetic nanoparticles. Eur Biophys J 2008;37:223–228.
49. Hergt R, Hiergeist R, Zeisberger M, Shüler D, Heyen U, Hilger I, Kaiser WA. Magnetic properties of bacterial magnetosomes as potential diagnostic and therapeutic tools. J Magn Magn Mater 2005;293:80–86.